

**Technical Conference for 60th Anniversary of Geology Department, Taida:  
Sustainable Development and Geoscience Perspective, 12/20/1999**

**Geochemistry of the hydrosphere in Taiwan**

(To the fond memory of Lee, Pei-jan)

Yuan-Hui Li

Department of Oceanography  
University of Hawaii, Honolulu  
Hawaii 96822

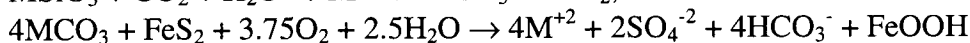
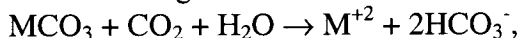
The factor analysis and geographical distribution patterns of the concentrations of major ions in rainwater, rivers, and lakes, provide important clues in the major processes that control the composition of those water bodies. The following presents a couple of examples from Taiwan.

The circles and triangles in Figure 1 are rainwater sampling sites that are supported by the Environment Protection Administration of Taiwan and the Taiwan Forestry Research Institute, respectively. King et al. (1994) and Chen et al. (1996) summarize the average composition of rainwater at those sites. The factor analysis results of those data, as shown in Figure 2a (factor loading), indicate that there are two major factors: Factor 1 ( $\text{Cl}^-$ ,  $\text{Na}^+$ ,  $\text{Mg}^{+2}$ , and partly  $\text{Ca}^{+2}$ ) mainly represents the seasalt input in rainwater. The concentrations of those ions are inversely correlated to the amount of rainfall. Factor 2 (non-seasalt  $\text{SO}_4^{-2}$ ,  $\text{NO}_3^-$ ,  $\text{NH}_4^+$ , and  $\text{H}^+$ ) represents the anthropogenic input, mainly from fossil fuel burning. The non-seasalt  $\text{SO}_4^{-2}$  ( $\text{nsSO}_4^{-2}$ ) is calculated by the relationship:  $\text{nsSO}_4^{-2} = \text{SO}_4^{-2} - (\text{SO}_4^{-2} / \text{Cl}^-)_{\text{seawater}} \times \text{Cl}^-$ . Ions within the same ellipse in Figure 2a have a correlation coefficient of greater than 0.5 between any pair of ions. As shown in Figure 2b (factor scores, numerals represent the sampling sites shown in Figure 1), the change in chemical composition of rainwater is mainly controlled by anthropogenic inputs. One obvious exception is station 10 (Peng-hu Island), which is greatly enriched in seasalt component. For comparison, station 12 (Ali-shan) contains the least amount of seasalt component. Station 8 (Tai-chung) has the highest anthropogenic component, and station 5 (Ken-ting) the lowest. The concentration of  $\text{K}^+$  is not correlated to that of any other major ions, and the seasalt component of  $\text{K}^+$  in rainwater is minor.

The xy-plots among  $\text{Cl}^-$ ,  $\text{Na}^+$ , and  $\text{Mg}^{+2}$  (Figures 3a and 3b) confirm the seasalt origin of those ions in rainwater. However, the concentration of  $\text{Na}^+$  tends to be slightly lower than the expected values from seawater, probably because of the calibration problem of  $\text{Na}^+$  analysis. The seasalt component of  $\text{Ca}^{+2}$  is small in rainwater (Figure 3c). The non-seasalt  $\text{Ca}^{+2}$  ( $\text{nsCa}^{+2}$ ) can be estimated by the formula:  $\text{nsCa}^{+2} = \text{Ca}^{+2} - (\text{Ca}^{+2} / \text{Cl}^-)_{\text{seawater}} \times \text{Cl}^-$ . The  $\text{nsCa}^{+2}$  is probably introduced into rainwater by dissolution of fine carbonate particles through natural and anthropogenic acids such as  $\text{H}_2\text{SO}_4$  and  $\text{HNO}_3$  in rainwater. The xy-plots among  $\text{nsSO}_4^{-2}$ ,  $\text{NO}_3^-$ , and  $\text{NH}_4^+$  (Figures 3d and 3e) show larger scattering, indicating additional sources for  $\text{NO}_3^-$  at stations 2, 10, m2, and m4; and for  $\text{NH}_4^+$  at stations 9 and m5; or they may simply be data noise. As shown in Figure 3f, the equivalents of  $\text{H}^+$  introduced by sulfuric and nitric acids ( $\text{NO}_3^- + \text{nsSO}_4^{-2}$ ) into rainwater is more or less balanced by consumption of  $\text{H}^+$  by  $\text{NH}_3$  and  $\text{CaCO}_3$  along with the leftover  $\text{H}^+$  in rainwater ( $\text{H}^+ + \text{NH}_4^+ + \text{nsCa}^{+2}$ ).

The spatial variation of  $\text{Cl}^-$  concentration in rainwater over Taiwan (Figure 4) shows low concentrations for the high mountain area, especially over station 12 (Alishan), and high concentrations for the western and eastern coastal areas. The implication is that a large fraction of seasalt aerosols carried by air masses is washed out by rainfall before reaching the high mountain or inland areas. The concentrations of  $\text{nsSO}_4^{-2}$ ,  $\text{NO}_3^-$ , and  $\text{nsCa}^{+2}$  are highest in the northwestern coastal area and tend to decrease toward the east (Figure 4). Therefore, the major anthropogenic sources for  $\text{SO}_4^{-2}$  and  $\text{NO}_3^-$  are located in Taiwan's northwestern coastal area. However, one should note that a large section of the eastern coast is devoid of sampling sites. High  $\text{NH}_4^+$  concentrations centered around stations 9, 8, 11, and 4 in the southwestern coastal area are likely to be related to the release of  $\text{NH}_3$  by numerous pig and duck farms in the area, in addition to the input from fossil fuel burning. The pH values are lowest at stations 1 (Taipei) and 4 (Kaohsiung), and are highest at station 9 (Tainan), which also has the highest  $\text{NH}_4^+$  concentration.

Factor analysis results of water composition data for about one hundred lakes and reservoirs in Taiwan (Li et al., 1997) are summarized in Figures 5a (factor loading) and 5b (factor score). The location of these water bodies are shown in Figure 7, as closed circles for altitudes greater than 500m, as open circles for altitudes less than 500m, and as x's for offshore islands. Since the residence time of water in Taiwan's lakes and reservoirs is generally less than three to four months, the following discussions should also apply to river water flowing into those lakes and reservoirs. Factor 1 (Alkalinity,  $\text{Ca}^{+2}$ ,  $\text{Mg}^{+2}$ , and  $\text{SO}_4^{-2}$ ) in Figure 5a represents the inputs from weathering of carbonates (marbles and limestones) and aluminosilicates (gneiss and schists), which may contain pyrite veins and grains, in the upstream drainage areas of those water bodies. The schematic weathering reactions are:



where M is Ca and Mg. According to the above reactions, the concentrations of seasalt-corrected  $\text{Ca}^{+2}$ ,  $\text{Mg}^{+2}$ ,  $\text{SO}_4^{-2}$  and alkalinity in lakes and reservoirs should be all linearly correlated as proven in Figures 6d, 6e, and 6f. Also, the equivalents of seasalt-corrected  $\text{Ca}^{+2} + \text{Mg}^{+2}$  should be balanced by those of  $\text{HCO}_3^- + \text{SO}_4^{-2}$ . This is the case for most of samples as shown in Figure 6c. Factor 2 ( $\text{Cl}^-$ ,  $\text{Na}^+$ , and  $\text{K}^+$ ) in Figure 5a may represent the input from rainwater and some additional input of  $\text{Na}^+$  from weathering processes, as indicated by a moderate correlation between  $\text{Na}^+$  and  $\text{Mg}^{+2}$  or alkalinity in the same figure. As also shown in Figure 6a, Taiwan's lakes and reservoirs have a large non-seasalt  $\text{Na}^+$  component. A large fraction of  $\text{K}^+$  in Taiwan's lakes and reservoirs is also non-seasalt but its magnitude is similar to that in rainwater (Figure 6b; as crosses). Therefore, the net input of  $\text{K}^+$  from weathering should be negligible. For reference, ratios of various ion pairs from the world's mean river water (Meybeck, 1987) are also shown as solid diagonal lines in Figure 6. The compositions of water samples from Taiwan's lakes and reservoirs do not differ much from that of world's mean river.

Factor 2 scores are consistently low for high altitude lakes (Figure 5b). This is consistent with the low concentration of  $\text{Cl}^-$  in the Central Range area as shown in Figure 7. The concentration of  $\text{Cl}^-$  increases from the Central Range toward the coastal areas, especially toward the most western coastal area, where rainfall is low and the evaporation

rate of water is highest in Taiwan. It is evident from Figure 5b that chemical weathering, as represented by factor 1, is the dominant natural process in controlling the water chemistry of Taiwan's rivers, lakes and reservoirs. Again, the concentrations of alkalinity and non-seasalt  $\text{SO}_4^{-2}$  (factor 2 ions) are low in the Central Range area, and highest in the most western coastal area (Figure 7).

### References

- Chen, C.S., Lin, N.H., Peng, C.M., and Jeng, F.T., Acidic deposition on Taiwan and associated precipitation systems, International Conference on Acid Deposition in East Asia, 124-132, 1996.
- King, H.B., Hsia, Y.J., Liou, C.B., Lin, T.C., Wang, L.J., and Hwong, J.L., Chemistry of precipitation, throughfall, streamflow and streamwater of six forest sites in Taiwan, in *Biodiversity and Terrestrial Ecosystems*, eds. C. I. Peng and C. H. Chou, 355-362, 1994.
- Li, Y.H., Chen, C.T. and Hung, J.J., Aquatic chemistry of lakes and reservoirs in Taiwan, *Terrestrial, Atmospheric and Oceanic Sciences* 8, 405-426, 1997.
- Meybeck, M., Global chemical weathering of surficial rocks estimated from river dissolved loads. *Am. J. Sci.* 287, 401-272, 1987.

Table 1: The correlation coefficient matrix for Taiwan's rainwater.

	Cl	H	K	Mg	Na	NH <sub>4</sub>	NO <sub>3</sub>	nsCa	nsSO <sub>4</sub>	rainfall
Cl	1									
H	-0.00	1								
K	0.11	-0.13	1							
Mg	<b>0.95</b>	0.12	-0.05	1						
Na	<b>0.94</b>	0.11	-0.13	<b>0.97</b>	1					
NH <sub>4</sub>	-0.29	0.38	0.00	-0.18	-0.17	1				
NO <sub>3</sub>	0.18	<b>0.55</b>	-0.02	0.26	0.21	<b>0.52</b>	1			
nsCa	0.46	-0.03	-0.13	<b>0.50</b>	0.46	0.29	<b>0.50</b>	1		
nsSO <sub>4</sub>	0.08	<b>0.66</b>	-0.12	0.21	0.21	<b>0.72</b>	<b>0.75</b>	0.49	1	
rainfall	-0.44	-0.12	-0.14	-0.48	-0.48	-0.09	-0.16	-0.18	-0.23	1

Table 2: Correlation coefficient matrix of the compositional data from Taiwan's lakes and reservoirs.

	Cl	Alk	SO <sub>4</sub>	NO <sub>3</sub>	Ca	Mg	K	Na	pH
Cl	1								
Alk	0.42	1							
SO <sub>4</sub>	0.21	<b>0.57</b>	1						
NO <sub>3</sub>	-0.01	0.25	-0.02	1					
Ca	0.24	<b>0.88</b>	<b>0.63</b>	0.35	1				
Mg	0.48	<b>0.77</b>	<b>0.69</b>	0.09	<b>0.61</b>	1			
K	0.48	0.38	0.31	-0.01	0.27	0.34	1		
Na	<b>0.93</b>	<b>0.55</b>	0.32	0.02	0.31	<b>0.58</b>	<b>0.55</b>	1	
pH	0.13	0.42	0.33	0.19	0.43	0.45	0.26	0.29	1

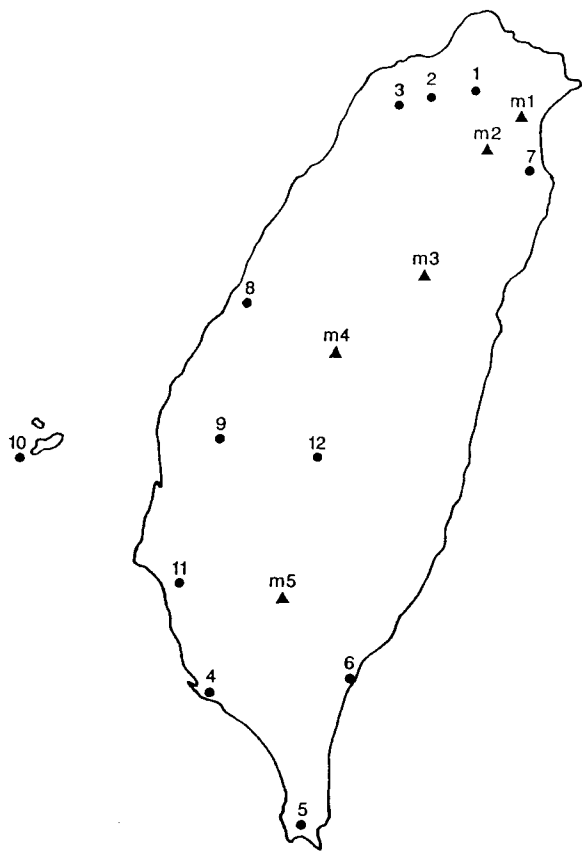


Figure 1: Rainwater sampling sites administered by the Environment Protection Administration of Taiwan (1-12) and by the Forestry Research Institute (m1-m5).

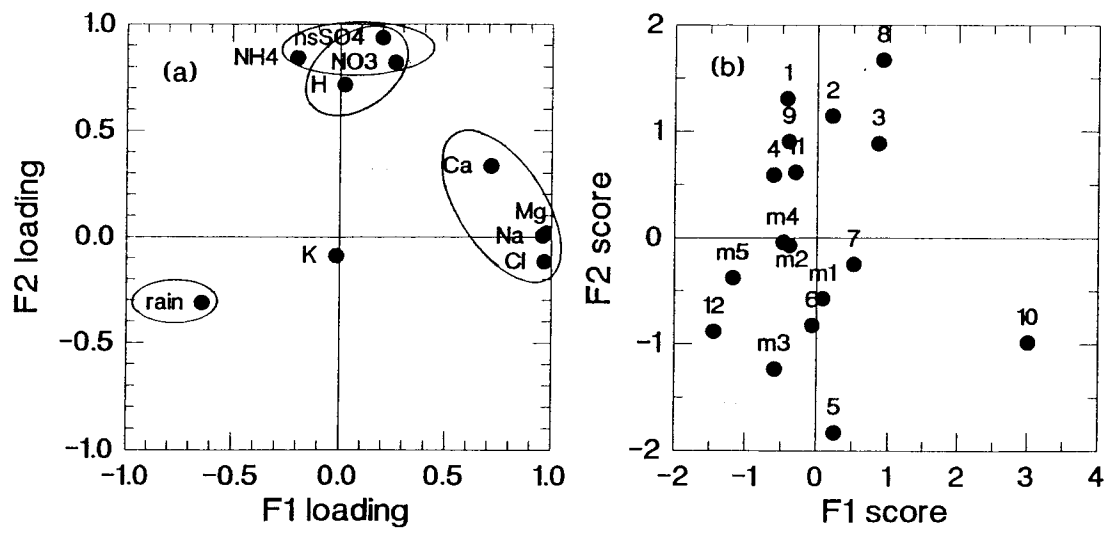


Figure 2: Factor loadings (a) and factor scores (b) of factors 1 and 2 obtained from the factor analysis of average rainwater data from the sampling sites given in Figure 1.

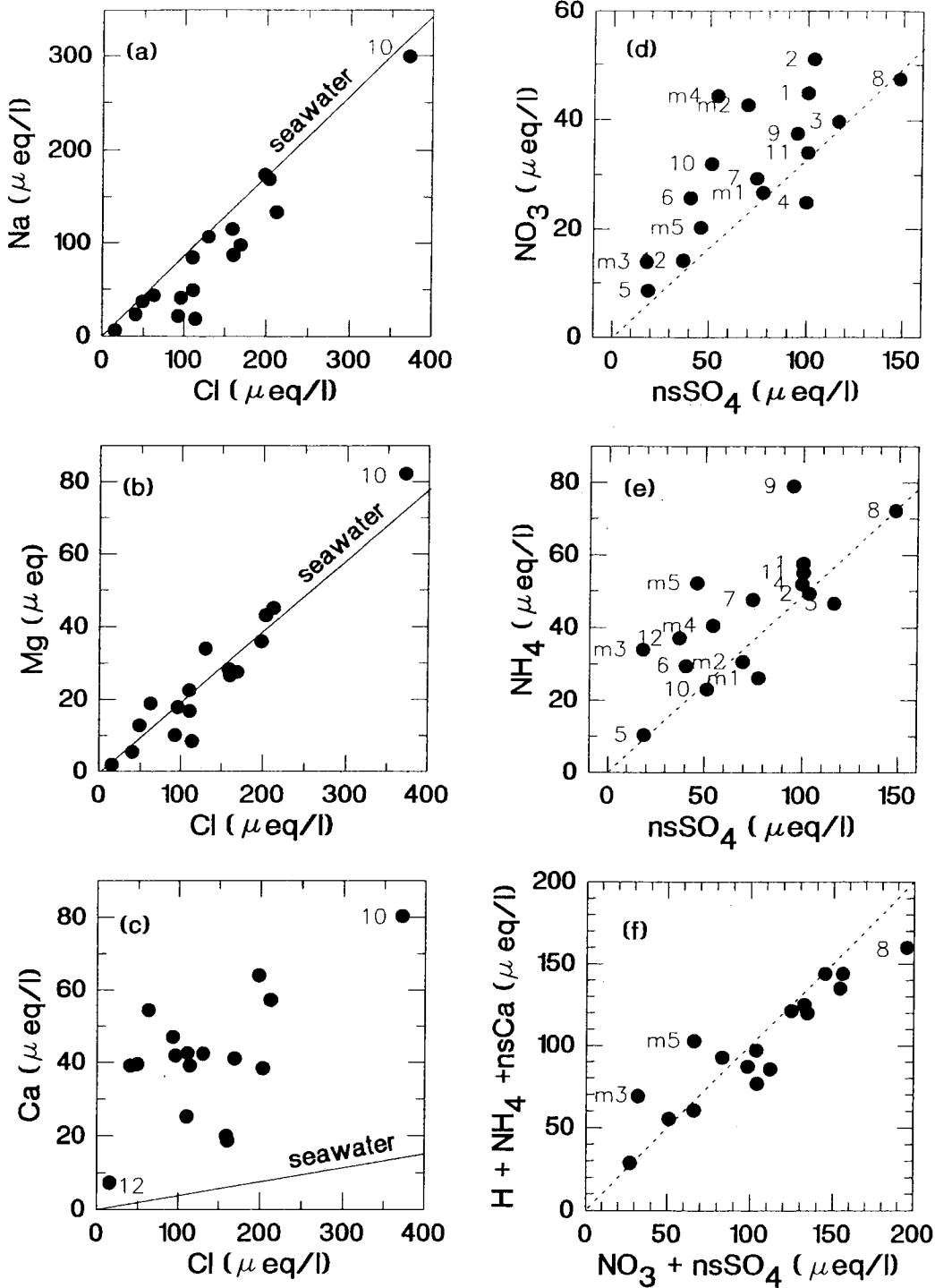


Figure 3: XY-plots of various ion concentrations in rainwater.

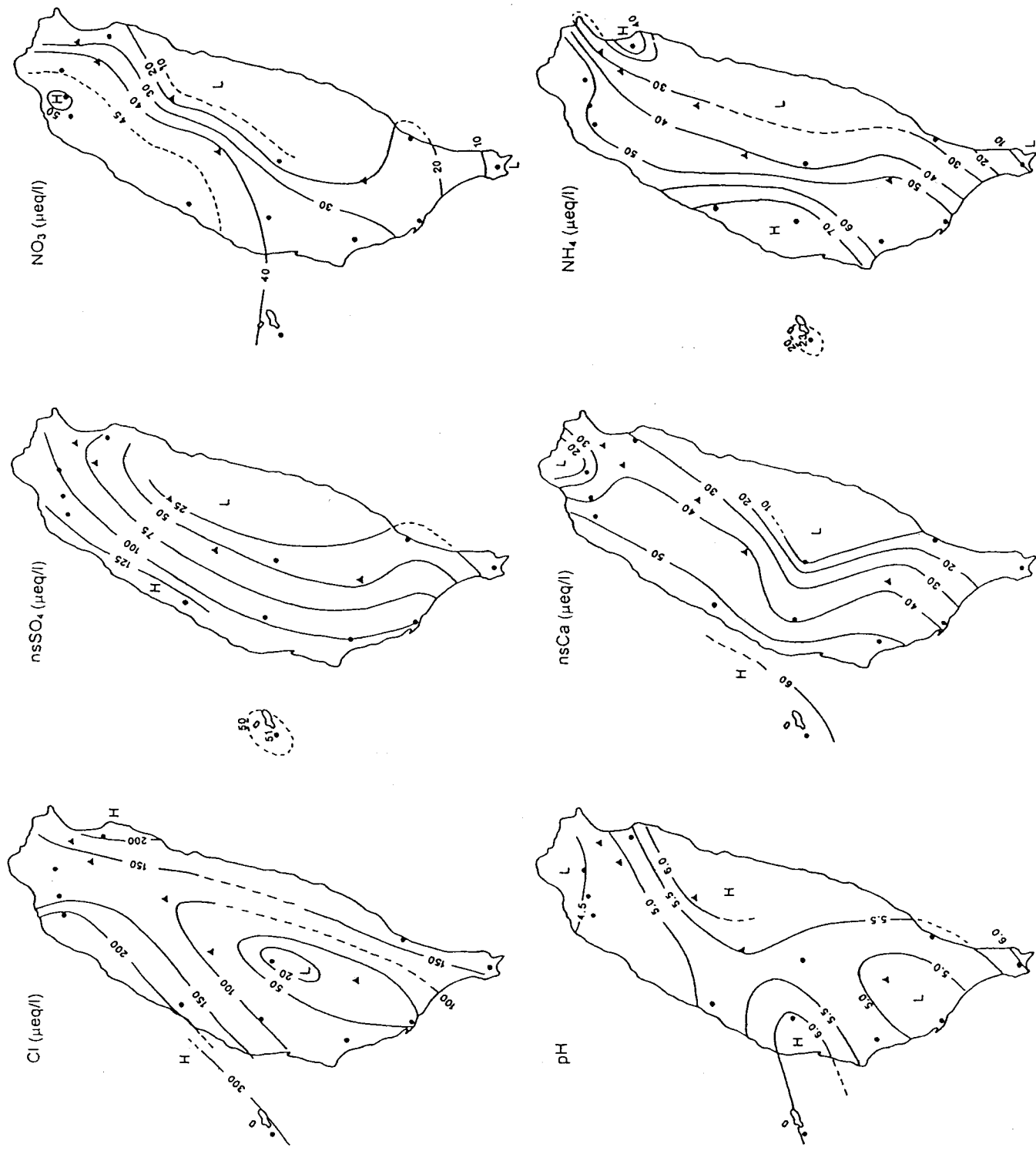


Figure 4: Spatial variations of average concentrations of various ions in rainwater.

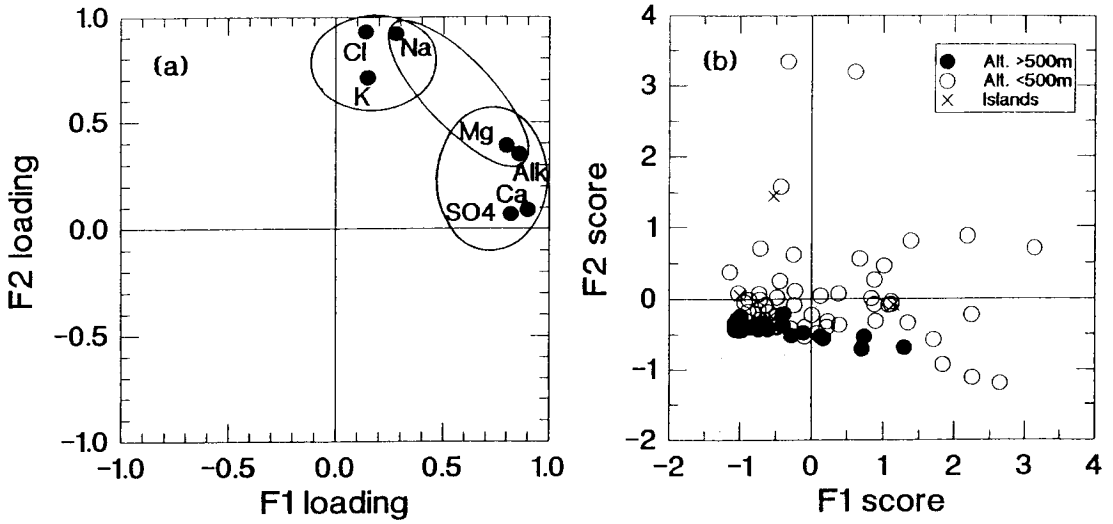


Figure 5: Factor loadings (a) and factor scores (b) of factors 1 and 2 obtained from the compositional data of lake waters from Taiwan with lake altitude greater (solid circles) and less (open circles) than 500 meters and from off shore islands.

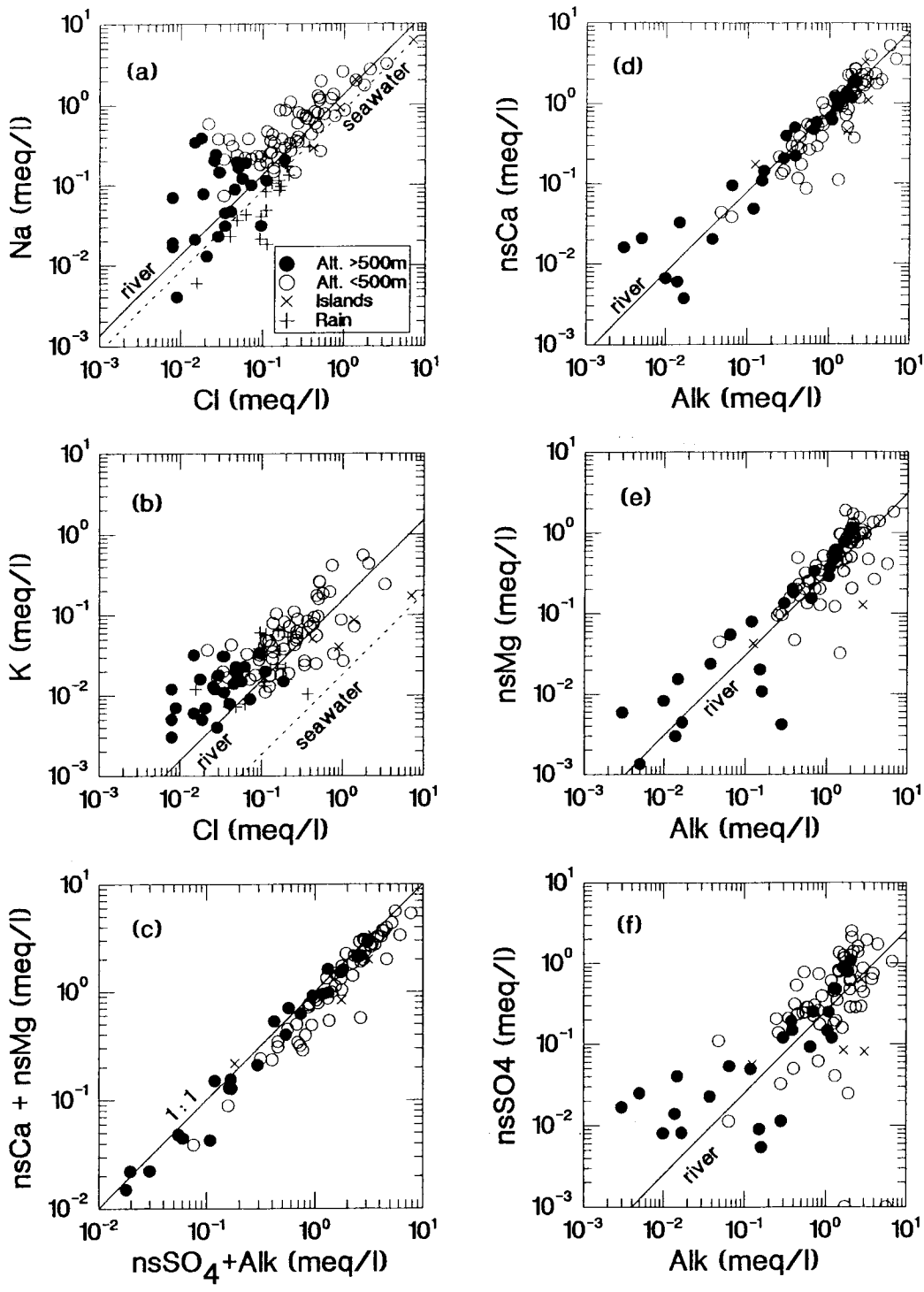


Figure 6: XY-plots of various ion concentrations in lakes and rainwater.

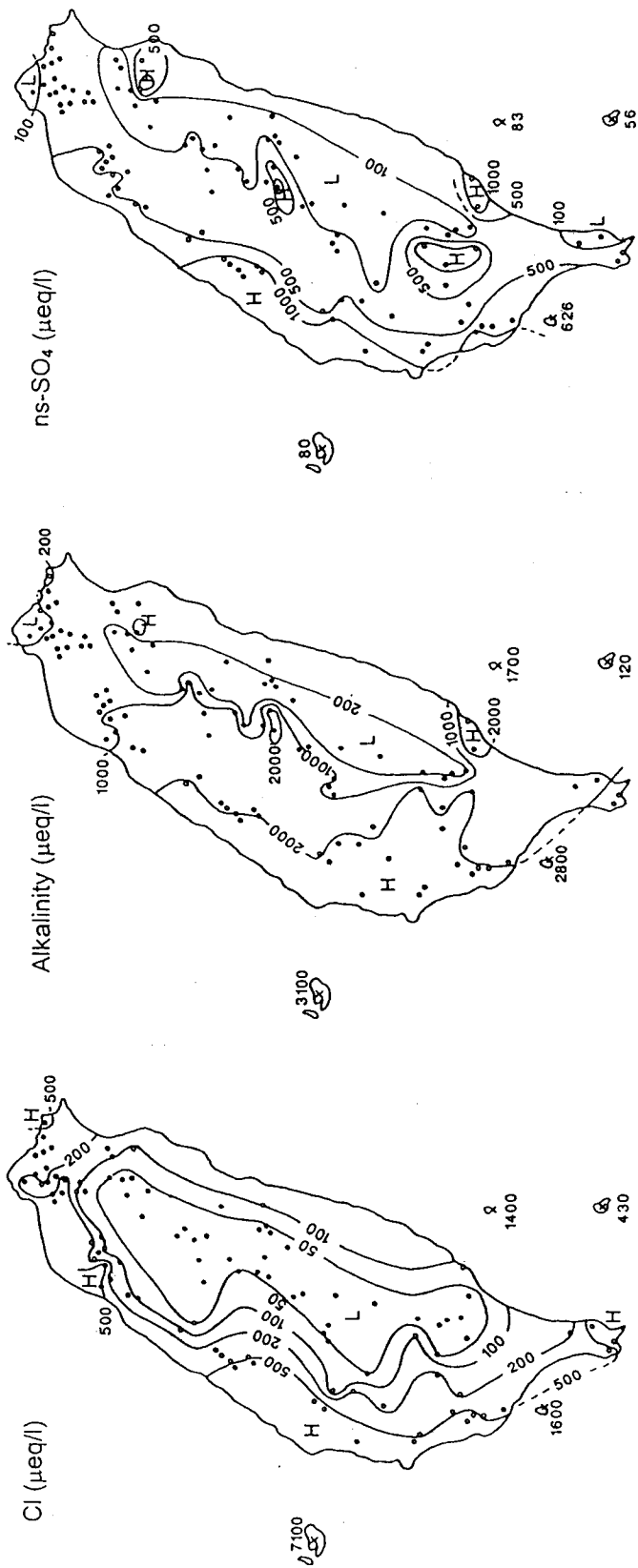


Figure 7: Spatial variations of Cl, alkalinity and non-seasalt SO<sub>4</sub> concentrations in lakes